BF-2029
[1-11]

RESEARCH ARTICLE Indian Journal of Animal Research

Evaluation of Atlas (C1) and Axis (C2) Morphometry in Aksaray Malakli Dogs with 3D Modeling Method

Muhammet Alperen Fidan[1], Zekeriya Özüdöğru[2], Ramazan İlgün[1]

10.18805/IJAR.BF-2029

ABSTRACT

Background: This study aimed to comprehensively evaluate the morphometric characteristics of the atlas (C1) and axis (C2) cervical vertebrae in Aksaray Malakli dogs. Using advanced three-dimensional (3D) surface scanning technology, the research provides detailed and breed-specific anatomical data for this unique dog breed.

Methods: Seven atlas and seven axis bones were collected from adult Aksaray Malakli dogs and scanned using a color 3D surface scanner. High-resolution digital models of each bone were generated and a total of 25 linear and one angular osteometric measurements were performed on each model using specialized 3D analysis software. To ensure measurement reliability, all parameters were measured three times by the same researcher and intra-observer agreement was high for both vertebrae [intraclass correlation coefficient (ICC) > 0.75].

Result: Descriptive statistics and correlation analyses identified significant structural relationships among several morphometric parameters. Comparative assessments demonstrated that certain morphometric features of Malaklı dogs differ considerably from those of other dog breeds and mammalian species. Notably, the dens-to-axis length ratio (DALR) and dens angle (DA^{o}) values provided critical insights into the predisposition of large breed dogs to atlantoaxial instability. Furthermore, the study confirmed the high reliability and repeatability of measurements obtained *via* 3D surface scanning. These findings establish essential baseline data for future anatomical investigations and offer novel comparative information on the morphometry of the Aksaray Malakli breed.

Key words: 3D surface scanning, Atlantoaxial instability, Large breed dog, Morphometry.

INTRODUCTION

Aksaray Malaklı dogs are native to Central Anatolia, particularly in the regions of Aksaray, Nevşehir and Şereflikoçhisar, Turkey (Atasoy *et al*., 2011). Owing to their characteristic drooping lips and cheeks, these dogs are commonly referred to as “Malakli,” meaning “with large cheeks.” Distinct genetic features of the breed include black spots on the head, grayish coat coloration, a large skull and a prominent drooping mouth and lip structure (Atasoy and Kanlı, 2005).

In recent years, three-dimensional (3D) surface models have become highly valuable in geometric morphometric studies across anatomy (Arya *et al*., 2024), osteoarchaeology and forensic sciences (Waltenberger *et al*., 2021; Özkadif *et al*., 2019; Fidancı and Orhan, 2025). 3D reconstructions permit precise morphometric measurements and qualitative morphological assessments without damaging original specimens and they also facilitate digital storage and sharing (Gelati and Tanga, 2015). Surface scanners use either laser or visible light to analyze object surfaces. While optical scanners offer sufficient color detail and resolution for distance measurements and landmark placement, laser scanners provide greater accuracy and perform better in daylight conditions, albeit without capturing tissue color information (Friess, 2012). Modern scanners tend to be lightweight, portable and suitable for handheld use (Adams *et al*., 2015).

The cervical vertebrae form the bony framework of the neck, supporting its weight and allowing for head movement (König and Bragulla, 2007). All domestic mammals possess seven cervical vertebrae (Akers and Denbow, 2013). The first, second, sixth and seventh cervical vertebrae are morphologically distinct from the others and are classified as “atypical cervical vertebrae” (Waxenbaum *et al*., 2025). Except for the atlas, the vertebral bodies are broad, narrowing towards the last cervical vertebra. The spinous process-a prominent dorsal projection found in most vertebrae-is relatively small and thin in the cervical region (Dyce *et al*., 2009). Due to their morphometric diversity and clinical importance, cervical vertebrae have been the subject of numerous studies (Zibis *et al*., 2016; Prameela *et al*., 2020), including those focused on surgical applications

[1]Department of Veterinary Anatomy, Faculty of Veterinary Medicine, Aksaray University, [68000], Aksaray, Turkey.
[2]Department of Veterinary Anatomy, Faculty of Veterinary Medicine, Balikesir University, [10000], Balikesir, Turkey.

Corresponding Author: Muhammet Alperen Fidan, Department of Veterinary Anatomy, Faculty of Veterinary Medicine, Aksaray University, [68000], Aksaray, Turkey.
Email: muhammetalperenfidan@aksaray.edu.tr
ORCIDs: 0000-0001-8408-3613, 0000-0002-0789-3628, 0000-0003-0150-3008.

How to cite this article: Fidan, M.A., Özüdöğru, Z. and Ilgün, R. (2025). Evaluation of Atlas (C1) and Axis (C2) Morphometry in Aksaray Malakli Dogs with 3D Modeling Method. *Indian Journal of Animal Research*. 1-11. doi: 10.18805/IJAR.BF-2029.

Submitted: 30-05-2025 **Accepted:** 07-09-2025 **Online:** 05-11-2025

(da Costa *et al*., 2008; Falzone *et al*., 2022), breed-specific comparative morphometry (Fourie and Kirberger, 1999) and evolutionary anatomy (Brocal *et al*., 2018). The cranium-C1 (atlanto-occipital) joint provides approximately half of the total cervical flexion/extension and the C1-C2 (atlanto-axial) joint provides approximately half of the rotation. The ala atlantis of the atlas transmits loads from the skull to the cervical spine, while the dens of the axis forms a pivot within the atlas ring, enabling head rotation (Kalantar, 2013). Morphological studies of canine cervical vertebrae are essential for clarifying breed differences and providing guidance for veterinary surgical procedures.

Investigating the morphometric characteristics of Aksaray Malaklı dogs is particularly important, as they serve as guardian dogs, are an integral part of regional livestock farming and represent a rare breed unique to a specific area. Although several studies have addressed various features of this breed (Fidan *et al*., 2024; ilgün *et al*., 2022; İlgün *et al*., 2017; İnanç *et al*., 2018), to date no comprehensive morphometric analysis of the atlas (C1) and axis (C2)-the atypical cervical vertebrae-has been conducted.

The primary aim of the present study was to evaluate the accuracy and reliability of morphometric and angular measurements obtained from 3D surface scanner models (Fig 1) of the atlas (C1) and axis (C2) vertebrae in Aksaray Malaklı dogs (Fig 2, Fig 3). Additionally, these digital reconstructions were compared with published data from other dog breeds to identify breed-specific anatomical differences.

MATERIALS AND METHODS

Collection of bones

This study used seven atlas and seven axis vertebrae (four males, three females) obtained from adult Aksaray Malaklı dogs, aged 5-8 years and weighing 60-75 kg. The specimens were collected from clinically healthy animals that died of natural causes between 2020 and 2025. Standard anatomical dissection procedures were followed: skin and subcutaneous tissues were first removed to expose the vertebral region. The surrounding muscles, ligaments and connective tissues were carefully dissected from the bones using scalpels and scissors. Intervertebral joints-capsules, ligaments and discs-were incised to isolate the atlas (C1) and axis (C2) from adjacent vertebrae. Any residual soft tissue was removed either mechanically or by soaking the bones in a moderate hydrogen peroxide solution to ensure clean surfaces for morphometric measurements. The specimens were catalogued accordingly. All procedures adhered to the guidelines of the Animal Ethics Committee at Aksaray University (approval no: 2025/23).

Surface scanning procedure

High-resolution, color surface models of each bone were obtained using a Revopoint POP 3 Plus Standard Edition scanner (Shenzhen, China) in color mode with default settings. Scans were conducted in a dark room to minimize ambient light and optimize image quality. The scanner was calibrated prior to each session according to the manufacturer's

(Abbreviations; 1, Tuberculum dorsale; 2, Processus transversus (ala atlantis); 3, Foramen transversarium; 4, Foramen vertebrale laterale; 5, Facies articularis caudalis; 6, Incisura alaris; 7, Foramen transversarium; 8, Processus transversus; 9, Processus spinosus; 10, Dens; 11, Facies articularis cranialis; 12, Processus articularis caudalis).

Fig 1: General morphological features of C1 (atlas) and C2 (axis) in Aksaray Malakli dogs.

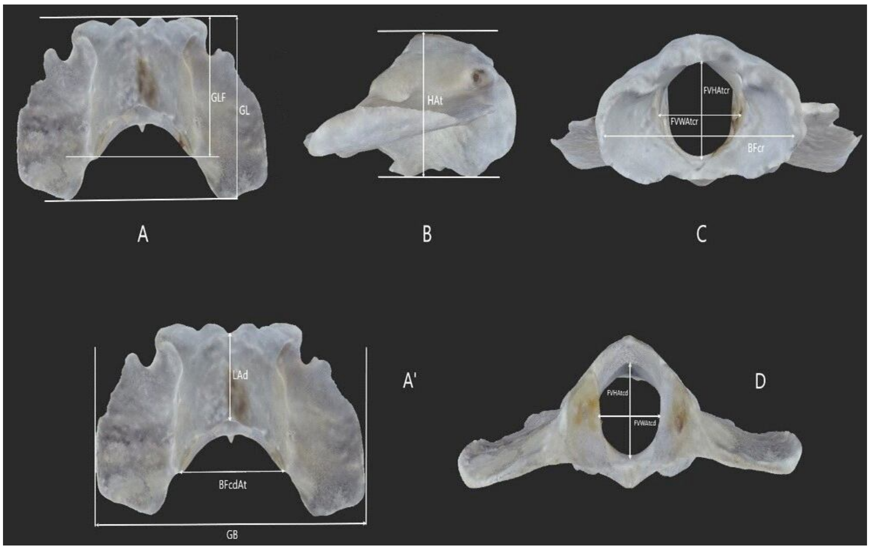

(Abbreviations; GB: Greatest breadth over the wings; GL: Greatest length; GLF: Greatest length from the cranial articular surface to the caudal articular surface; LAd: Length of the dorsal arc; HAt: Height of the atlas; BFcr: Greatest breadth of the cranial articular surface; BFcdAt: Greatest breadth of the caudal articular surface of the atlas; FVHAtcr: Height of the cranial vertebral foramen of the atlas; FVHAtcd: Height of the caudal vertebral foramen of the atlas; FVWAtcr: Wdth of the cranial vertebral foramen of the atlas; FVWAtcd: Width of the caudal vertebral foramen of the atlas; A and A': Dorsal view of the atlas; B: Lateral view of the atlas; C: Cranial view of the atlas; D: Daudal view of the atlas).

Fig 2: Osteometric measurement points and 3D morphology of the atlas in Aksaray Malakli dogs.

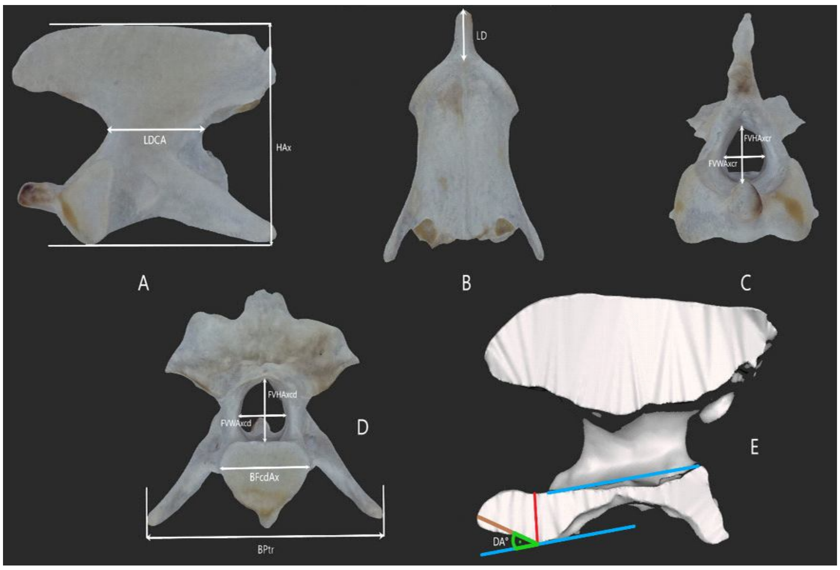

(Abbreviations; LDCA: Length of the dorsal canal axis; BPtr: Greatest breadth across the transverse processes; BFcdAx: Greatest breadth of the caudal articular surface of the axis; HAx: Height of the axis; DA°: Dens angle; LD: Length of the dens; DALR: Dens to axis length ratio; FVHAxcr: Height of the cranial vertebral foramen of the axis; FVHAxcd: Height of the caudal vertebral foramen of the axis; FVWAxcr: Width of the cranial vertebral foramen of the axis; FVWAxcd: Width of the caudal vertebral foramen of the axis; A: Lateral view of the axis; B: Ventral view of the axis; C: Cranial view of the axis; D: Caudal view of the axis; E: Sagittal section view of the axis).

Fig 3: Osteometric measurement points and 3D morphology of the axis in Aksaray Malakli dogs.

instructions. Images were processed with Revo Scan v5.5.2 software and exported in OBJ format. Each atlas and axis model was subsequently analyzed using Meshmixer (v3.5). The digital models were cross-checked against the original bones and standard anatomical references (Evans and De Lahunta, 2012; Barone, 1999) and manual corrections were made whenever necessary to ensure validation.

Morphometric analysis

All OBJ files were imported into 3D Slicer (v5.6.2) (Fedorov *et al*., 2012) , where 25 linear and one angular measurement were performed on each bone. Detailed osteometric landmarks are provided in Table 1 and 2 (Von Den Driesch, 1976). The dens angle (DA°) of the axis was measured as described by Takahashi *et al*. (2017). For this, 3D models were sagittally bisected in Meshmixer and the angle between the floor of the vertebral canal and the dens was measured in ImageJ (v1.54). All measurements were completed by a single researcher. To assess intra-observer repeatability and reduce measurement bias, each measurement was repeated three times at different intervals in a blinded fashion and the average value was used for analysis. Thus, reliability and objectivity were ensured. All anatomical terms conform to the Veterinaria (2017).

Statistical analysis

Statistical analyses were conducted using SPSS version 29.0. Descriptive statistics (mean, standard deviation, minimum and maximum) were calculated for all parameters. Relationships between continuous variables were assessed using the Pearson correlation coefficient; when parametric assumptions were not met, Spearman's correlation was applied. Statistical significance was set at $p<0.05$ and $p<0.01$. Intra-observer reliability was assessed using the Intraclass Correlation Coefficient (ICC) with 95% confidence intervals (McGraw and Wong, 1996; Longo *et al*., 2018). Sex based differences (sexual dimorphism) were not evaluated due to the limited availability of specimens from this rarely bred, endemic dog breed, which precluded balanced male–female sampling.

RESULTS AND DISCUSSION

The morphometric features of the atlas and axis in Aksaray Malakli dogs were evaluated by performing three repeated measurements on each 3D model. Intraclass correlation coefficients (ICCs) were all statistically significant and exceeded 0.75, indicating high measurement reliability (Table 3). For the atlas, ICC values ranged from 0.921 to

Table 1: Morphometric parameters and descriptive definitions for atlas in Aksaray Malakli dogs.

Parameters	Definition of measurements	Description of measurements
GB	Greatest breadth over the wings	The distance between the two most lateral points of the processus transversi.
GL	Greatest length	The length between the most cranial point and the most caudal point of the Atlas
GLF	Greatest length from the facies articularis cranialis to the facies articularis caudalis	From the cranialmost point of the facies articularis cranialis to the caudalmost point of the facies articularis caudalis
LAd	Length of the dorsal arc	From the cranialmost point of the arcus dorsalis to the caudalmost point.
HAt	Height of the atlas	Distance between the most dorsal point of the dorsal arc and the most ventral point of the ventral arc.
BFcr	Breadth (greatest) of the facies articularis cranialis	The greatest breadth of the cranial articular facies.
BFcdAt	Breadth (greatest) of the facies articularis caudalis of the atlas	The greatest breadth of the caudal articular facies.
FVHAtcr	Height of the cranial foramen vertebrale of the atlas	The cranialmost point to the caudalmost point of the roof of the foramen vertebrale from cranial view.
FVHAtcd	Height of the caudal foramen vertebrale of the atlas	The cranialmost point to the caudalmost point of the roof of the foramen vertebrale from caudal view.
FVWAtcr	Width of the cranial foramen vertebrale of the atlas	The laterolateral widest point of the foramen vertebrale from cranial view.
FVWAtcd	Width of the caudal foramen vertebrale of the atlas	The laterolateral widest point of the foramen vertebrale from caudal view.
SAAt	Surface area of the atlas	
VAt	Volume of the atlas	

0.999, while for the axis, they ranged from 0.769 to 0.998. All parameters demonstrated ICC values above 0.75, a threshold considered satisfactory. The lowest ICC was observed for the dens-to-axis length ratio (DALR) of the axis (0.769) (Table 3).

The mean height of the axis (HAx) was 53.21±5.54 mm, which was higher than the mean height of the atlas (HAt) at 36.67±3.50 mm. Several atlas parameters-including the breadth of the caudal articular surface (BFcdAt), height of the cranial vertebral foramen (FVHAtcr), height of the caudal vertebral foramen (FVHAtcd), width of the cranial vertebral foramen (FVWAtcr) and width of the caudal vertebral foramen (FVWAtcd)-were greater than their axis counterparts (BFcdAx, FVHAxcr, FVHAxcd, FVWAxcr, FVWAxcd). Additionally, the mean surface area and total volume were higher for the axis (surface area: 13,101.33±2,633.01 mm²; volume: 29,331.98±8,153.71 mm³) compared to the atlas (surface area: 12,047.94±1,842.67 mm²; volume: 25,037.09±6,636.64 mm³) (Table 3).

Correlation analyses among the 3D-measured parameters for the atlas and axis are presented in Table 3 and 4. The greatest breadth of the atlas wings (GB), its surface area (SAAt) and its volume (VAt) all showed strong positive correlations (*e.g.*, GB and SAAt: r = 0.976, $p<0.01$; GB and VAt: r = 0.921, $p<0.01$). GB was also highly correlated with atlas height (HAt, r = 0.953, $p<0.01$) and the greatest breadth of the cranial articular surface (BFcr, r = 0.900, $p<0.01$). Significantly, the strong positive association between GB and SAAt indicates that as the atlas wings (ala atlantis) widen, the atlas surface area-and concomitantly its volume-increases proportionally, suggesting that lateral expansion of the wings is a primary contributor to overall atlas size.

The greatest length of the atlas (GL) and the distance from the cranial to caudal articular surfaces (GLF) both showed strong positive associations with surface area (SAAt) and volume (VAt), particularly with surface area (GLF and SAAt: r = 0.956, $p<0.01$). The BFcr value was also highly correlated with both surface area (SAAt: r = 0.927, $p<0.01$) and volume (VAt: r = 0.877, $p<0.01$) (Table 4).

Pearson correlation was used to assess the relationships and the analysis was verified for consistency with our predefined criteria. Breadth of the caudal articular surface of the atlas (BFcdAt) was strongly correlated with the height of both the cranial (FVHAtcr, r = 0.907, $p<0.01$) and caudal (FVHAtcd, r = 0.911, $p<0.01$) vertebral foramina (Table 4). The length of the dorsal arch (LAd) also showed positive correlations with surface area and volume, although correlations with other parameters were generally weaker. Overall, surface area (SAAt) and volume (VAt) demonstrated strong associations with multiple morphometric features of the atlas (Table 4).

Table 2: Morphometric parameters and descriptive definitions for axis in Aksaray Malakli dogs.

Parameters	Definition of measurements	Description of measurements
LDCA	Length of dorsal canal axis	Length of canal roof of parallel to canal
BPtr	Greatest breadth across the processus transversi	The distance between the two most lateral points of the processus transversi.
BFcdAx	Breadth (greatest) of the facies articularis caudalis of the axis	Laterolaterally distance between the two widest points of the facies articularis caudalis.
HAx	Height of the axis	Distance between the most dorsal point of the spinous process and the most ventral point of the corpus.
DA°	Dens angle	The angle between the floor of the vertebral canal and the ventral floor of the dens.
LD	Length of the dens	The length from the most proximal end of the dens to the most distal end of the dens.
DALR	Dens to axis length ratio	The ratio of the length of the dens to length of the axis body
FVHAxcr	Height of the cranial foramen vertebrale of the axis	The cranialmost point to the caudalmost point of the roof of the foramen vertebrale from cranial view.
FVHAxcd	Height of the cranial foramen vertebrale of the axis	The cranialmost point to the caudalmost point of the roof of the foramen vertebrale from caudal view.
FVWAxcr	Width of the cranial foramen vertebrale of the axis	The laterolateral widest point of the foramen vertebrale from cranial view.
FVWAxcd	Width of the cranial foramen vertebrale of the axis	The laterolateral widest point of the foramen vertebrale from caudal view.
SAAx	Surface area of the axis	
VAx	Volume of the axis	

For the axis, Pearson correlation analysis indicated significant positive relationships among several parameters (Table 5). The length of the dorsal canal axis (LDCA) was strongly correlated with both the surface area (SAAx, r = 0.904, p<0.01) and volume (VAx, r = 0.864, p<0.05) of the axis, as well as with its height (HAx, r = 0.900, p<0.01). The greatest breadth across the transverse processes (BPtr) also showed strong correlations with surface area (r = 0.973, p<0.01) and volume (r = 0.970, p<0.01). Similarly, axis height (HAx) was positively correlated with both SAAx and VAx. The length of the dens (LD) was significantly correlated with both surface area and volume. The width of the cranial vertebral foramen of the axis (FVWAxcr) was significantly associated with BPtr (r = 0.762, p<0.05) and SAAx (r = 0.728). As in the atlas, both surface area (SAAx) and volume (VAx) of the axis demonstrated strong correlations with a variety of morphometric features (Table 5).

Notably, DALR showed weak-to-moderate and generally non-significant correlations with the other morphometric variables, indicating that it does not systematically increase or decrease in tandem with morphometric lengths and functions largely as a size-independent ratio.

Previous research on the Aksaray Malakli breed has mainly investigated general anatomical features or linear measurements of long bones (Özüdoğru *et al*., 2023; Fidan, 2023). However, there is a notable lack of breed-specific morphometric data on the atlas and axis vertebrae, which are crucial for understanding cervical biomechanics in large dog breeds. In the present study, we utilized 3D modeling to achieve highly accurate, reproducible morphometric measurements of these vertebrae, thus establishing a methodological foundation for both clinical and research applications. Comparative data for the atlas and axis in various species are summarized in Tables 6 and 7.

Table 3: Morphometric features of the atlas and axis of the Aksaray Malakli dogs (N=7).

ATLAS			AXIS		
Parameters (mm)	Mean±SD (Min-Max)	ICC	Parameters (mm)	Mean±SD (Min-Max)	ICC
GB	108.92±9.33	0.999	LDCA	28.91±3.08	0.975
GL	57.31±3.17	0.921	BPtr	55.28±5.14	0.998
GLF	41.72±3.32	0.954	BFcdAx	22.49±2.82	0.820
LAd	23.84±1.87	0.972	HAx	53.21±5.54	0.987
HAt	36.67±3.50	0.972	DA°	31.89±5.76	0.972
BFcr	46.93±2.78	0.987	LD	14.49±1.64	0.956
BFcdAt	38.05±3.49	0.984	DALR	0.29±0.02	0.769
FVHAtcr	22.58±1.72	0.959	FVHAxcr	15.36±1.58	0.943
FVHAtcd	23.54±1.56	0.984	FVHAxcd	13.55±2.06	0.973
FVWAtcr	24.43±1.93	0.993	FVWAxcr	14.66±2.11	0.969
FVWAtcd	23.61±2.31	0.958	FVWAxcd	13.09±1.33	0.988
SAAt (mm^2)	12047.94 ±1842.67	-	SAAx (mm^2)	13101.33±2633.01	-
VAt (mm^3)	25037.09 ±6636.64	-	VAx (mm^3)	29331.98±8153.71	-

ICC < 0.5 poor reliability, 0.5 ≤ ICC<0.75 moderate reliability, 0.75 ≤ ICC < 0.9 good reliability and ICC ≤ 0.9 excellent reliability.

Table 4: Pearson Correlation test result between the parameters of the 3D modeled atlases.

	GB	GL	GLF	LAd	HAt	BFcr	BFcdAt	FVHAtcr	FVHAtcd	FVWAtcr	FVWAtcd	SAAt
GB												
GL	.864*											
GLF	.943**	.865*										
LAd	.833*	0.685	0.698									
HAt	.953**	.874*	.863*	.847*								
BFcr	.900**	.963**	.956**	0.664	.850*							
BFcdAt	.890**	.817*	.841*	0.561	.903**	.820*						
FVHAtcr	0.634	0.650	0.581	0.210	0.672	0.609	.907**					
FVHAtcd	0.661	0.556	0.634	0.212	0.660	0.578	.911**	.957**				
FVWAtcr	0.617	0.594	0.639	0.311	0.721	0.589	.835*	.795*	.842*			
FVWAtcd	0.470	0.450	0.445	0.178	0.615	0.405	.766*	.813*	.840*	.965**		
SAAt	.976**	.882**	.956**	.874*	.929**	.927**	.801*	0.493	0.515	0.549	0.366	
VAt	.921**	.815*	.902**	.884**	.828*	.877**	0.657	0.318	0.338	0.329	0.127	.969**

** p<0.01 / * p<0.05.

Our results demonstrate that the atlas and axis of Aksaray Malaklı dogs are morphologically distinct from those of smaller domestic breeds and other mammals. 3D modeling significantly increased the reliability and reproducibility of our measurements, consistent with the growing evidence supporting 3D imaging in veterinary anatomy (Smith and Jones, 2016; Hildebrand, 2019). Such precision is especially important for generating breed-specific reference data that can inform future anatomical, surgical and diagnostic work.

Comparative analysis shows the greatest breadth (GB) of the atlas in Malaklı dogs (108.92±9.33 mm) is, as expected, less than that found in animals such as cattle and horses, but much greater than in smaller species such as Persian cats (Derakhshi *et al*., 2024) and baboons (Tominaga *et al*., 1995). Including a range of other species in the comparison highlights how vertebral dimensions adapt to varying biomechanical demands across mammals (Table 6).

Within canines, our data indicate that Malaklı dogs, like other large breeds, exhibit clear differences from small and toy breeds-particularly in atlas width and other clinically relevant morphometric ratios (*e.g.*, DALR). For example, the mean GB and HAt values for Malaklı dogs are not only higher than those in Persian and Van cats, but also consistent with the expectation that larger breeds have more robust cervical vertebrae. These differences may influence vulnerability to cervical disorders, tolerance to injury and surgical considerations.

Regarding the axis, the sagittal diameter (*e.g.*, FVHAxcr, FVHAxcd) in Aksaray Malaklı dogs was greater than the transverse diameter-a trend seen in sheep and foxes, but not in all species (such as Van cats, baboons, or humans). In large breeds, a relatively larger sagittal diameter may reinforce the vertebra against greater forces associated with head movement, which is especially relevant for working on guardian breeds like the Malaklı (Table 7).

Dens hypoplasia-a key factor in atlantoaxial instability (AAI), especially in small breeds-can be evaluated using the dens-to-axis length ratio (DALR). Prior studies report DALR values of 0.41±0.12 in dogs overall, 0.36±0.009 in AAI-affected dogs and 0.40±0.007 in healthy controls (Takahashi *et al*., 2017); other studies have reported similar or lower values in affected dogs (Cummings *et al*., 2018; Kim *et al*., 2022; Planchamp *et al*., 2022). The DALR observed in Malakli dogs was 0.29±0.02-lower than typical reference ranges and similar to values found in AAI-affected dogs-suggesting a potential predisposition to AAI, though reference values specific to large breeds remain to be fully established.

The dens angle (DA°) is another key measurement for AAI diagnosis (Takahashi *et al*., 2017). DA° for toy breeds with AAI averages 41.0°±1.0°, significantly higher than in healthy toy breeds (37.6°±0.7°) and healthy Beagles (34.8°±0.5°). In Malakli dogs, the DA was 31.89°±5.76°, lower than reported for both healthy Beagles and toy breeds, suggesting a lower risk of AAI in this breed. However, more comparative morphometric data are needed to clarify the clinical significance of these values for large breeds.

Table 5: Pearson Correlation test result between the parameters of the 3D modeled axes.

	LDCA	BPtr	BFcdAx	HAx	DA°	LDDALR	FVHAxcr	FVHAxcd	FVWAxcr	FVWAxcd	SAAx	VAx
LDCA												
BPtr	.815*											
BFcdAx	0.588	0.475										
HAx	.900**	.877**	0.537									
DAo	-0.514	-0.107	0.142	-0.298								
LD	.802*	.852*	.819*	.783*	-0.071							
DALR	0.244	0.635	0.595	0.492	0.630	0.667						
FVHAxcr	0.726	0.553	0.566	0.534	-0.130	0.534	0.195					
FVHAxcd	.787*	0.675	0.459	0.680	-0.168	0.537	0.237	.904**				
FVWAxcr	0.616	.762*	0.509	0.562	0.175	0.649	0.563	.849*	.772*			
FVWAxcd	0.693	0.715	0.480	0.481	-0.103	0.668	0.307	.862*	.775*	.908**		
SAAx	.904**	.973**	0.577	.951**	-0.190	.875**	0.584	0.626	0.752	0.728	0.685	
VAx	.864*	.970**	0.395	.939**	-0.292	.797*	0.506	0.490	0.643	0.638	0.604	.970**

** p< 0.01 / * p< 0.05.

Table 6: Morphometric analysis of atlas in various mammalian species: A comparative review of literature (mm).

Study	Year	Species	Methods	N	Sex	GB	HAt	BFcr	FVHAtcr	FVHAtcd	FVWAtcr	FVWAtcd
Zehtabvar	2022	Cattle	CT	5	M	121.20±8.30						
et al.		Horse	CT	5	M	159.20±4.90						
Tominaga	1995	Human	Osteometric	6	-	85.20±4.50	50.00±1.00		17.00±		18.20±	
et al.		Baboon	Osteometric	9	-	47.30±4.80	25.40±2.40		1.20		1.30	
Şengül and	2006	Human	Osteometric	40	-	74.60±9.70		48.60±				
Kadioğlu								2.90				
Sharma and	2017	Human	Osteometric	50	-				29.91±	28.81±	26.56±	26.92±
Kumar									2.60	2.20	2.10	2.50
Derakhshi	2024	Persian	Osteometric	10	5 M	M: 29.39±	M: 13.59±		M: 9.09±	M: 9.08±	M: 9.81±	M: 6.64±
et al.		cats			5 F	0.67	0.51		0.25	0.30	0.25	0.25
						F: 29.22±	F: 13.27±		F: 8.95±	F: 8.92±	F: 9.69±	F: 9.52±
						0.61	0.53		0.20	0.31	0.30	0.37
Elasan and		Van							M: 9.33±	M: 5.63±	M: 11.61±	M: 8.92±
Yılmaz	2021	cats	CT	16	8 M				0.15	0.30	0.66	0.36
					8 F				F: 9.01±	F: 5.34±	F: 11.26±	F: 9.67±
									0.32	0.13	0.78	0.39
Current	2025	Aksaray	Surface	7	4 M	108.92±	36.67±	46.93±	22.58±	23.54±	24.43±	23.61±
Research		Malaklı	Scan		3 F	9.33	3.50	2.78	1.72	1.56	1.93	2.31
		dogs										
Study	Year	Species	Methods	N	Sex	GB	HAt	BFcr	FVHAtcr	FVHAtcd	FVWAtcr	FVWAtcd

Table 7: Morphometric analysis of axis in various mammalian species: A comparative review of literature (mm).

Study	Year	Species	Methods	N	Sex	LCDA	BPtr	HAx	DA°	LD	DALR	FVHAxcr
Wilke *et al.*	1995	Sheep	Osteometric	5	F							16.90±1.40
Tominaga	1995	Human	Osteometric	6	-		58.40± 3.40	54.80± 1.00		12.90± 0.80		
et al.		Baboon	Osteometric	9	-		33.00± 4.10	36.90± 4.10		7.00± 0.70		10.04±1.1
Şengül and Kadıoğlu	2006	Human	Osteometric	40	-					14.50± 2.30		
Özkadif and Haligür	2019	Fox	Osteometric	6								
Sharma and Kumar	2017	Human	Osteometric	50	-							19.06±1.83
Derakhshi *et al.*	2024	Persian cats	Osteometric	10	5 M 5 F		M: 13.32 ± 0.41 F: 13.17±0.41	M: 16.39± 0.67 F: 16.11±0.57		M: 4.44± 0.24 F: 4.27±0.19		M: 7.19± 0.24 F: 7.05±0.21
Elasan and Yılmaz	2021	Van cats	CT	16	8 M 8 F							M: 6.26± 0.29 F: 6.61± 0.29
White *et al.*	2019	Mixed dog breeds	CR	30	18 M 12 F	16.60± 2.80						
Cummings *et al.*	2018	Toy breed dogs	CR	70	-					C: 5.80 AI: 2.10	C:0.25 AAI: 0.14	
Planchamp *et al.*	2019	Beagle	CT	5	3 M 2 F					10.60		
Takahashi *et al.*	2017	Toy Breed dogsBeagle	CT	160	95 M 65 F				AAI: 41.0°± 1.0° NonAAI: 0.36°±0.7°		AAI: 37.6°±0.009 Non AAI: 0.40 ±0.007	
Kim *et al.*	2022	Maltese	CT	45	28 M 17 F						AAS: 0.31±0.06 Non AAS : 0.36±0.05	
Takahashi *et al.*	2017	Small breed dogs	CT	106	51 M 55 F						0.41±0.12 C: 0.39	
Planchamp *et al.*	2022	Small breed dogs	CT / MRI	28							AAI: 0.34	
Current Research	2025	Aksaray Malaklı dogs	Surface Scan	7	4 M 3 F	28.91± 3.08	55.28± 5.14	53.21± 5.54	31.89± 5.76	14.49± 1.64	0.29± 0.02	15.36± 1.58
Study	Year	Species	Methods	N	Sex	LCDA	BPtr	HAx	DA°	LD	DALR	FVHAxcr

Recent work by Lievens *et al*. (2025) compared MSCT, CBCT and optical white light desktop scanning (OWLDS) for cranial modeling, concluding that OWLDS produces highly accurate, repeatable 3D models without the need for segmentation (mean deviation 0.04/ mm versus MSCT). These findings support the value of optical scanning for reliable morphometric analysis, due to its operator-independence, lack of radiation and efficiency.

LIMITATIONS

This study has several limitations. The relatively small sample size and unequal sex distribution (four males and three females) limit the capacity for comprehensive statistical comparisons and may reduce the generalizability of the findings. Because this breed is endemic and rarely bred, obtaining specimens was challenging, which further constrained sample size. Additionally, while correlation analysis is useful, many variables tend to move in the same direction, potentially masking underlying structures or key trends. Therefore, the use of multivariate approaches such as Principal Component Analysis (PCA) or regression models in future studies with larger, more balanced cohorts may be valuable for revealing hidden clusters or fundamental patterns and for confirming and expanding upon these results.

CONCLUSION

3D surface scanning is a reliable and repeatable technique for morphometric analysis of canine vertebrae when standardized protocols are followed. This approach is well suited for anatomical studies. The morphometric baseline data provided here for Aksaray Malaklı dogs enrich the current literature and lay the groundwork for future comparative research involving large dog breeds.

ACKNOWLEDGEMENT

The present study was not supported by any funding sources.

Disclaimers

The views and conclusions expressed in this article are solely those of the authors and do not necessarily represent the views of their affiliated institutions. The authors are responsible for the accuracy and completeness of the information provided, but do not accept any liability for any direct or indirect losses resulting from the use of this content.

Informed consent

All procedures were approved by the Aksaray University Ethics Committee.

Conflict of interest

The authors declare that there are no conflicts of interest regarding the publication of this article. No funding or sponsorship influenced the design of the study, data collection, analysis, decision to publish, or preparation of the manuscript.

REFERENCES

Adams, J.W., Olah, A., McCurry, M.R., Potze, S. (2015). Surface model and tomographic archive of fossil primate and other mammal holotype and paratype specimens of the Ditsong National Museum of Natural History, Pretoria, South Africa. *PLoS ONE*. **10(10):** e0139800.

Akers, R.M., Denbow, D.M. (2013). Anatomy and Physiology of Domestic Animals. John Wiley and Sons.

Arya, M., Tyagi, S.P., Kumar, A., Kumar, A., ve Kumar, S. (2024). Radiographic mensuration of caudal vena cava, aorta, vertebral length and fourth rib width and ascertaining their ratios in healthy dogs. *Indian Journal of Animal Research*. **58(10):** 1718-1721. doi: 10.18805/IJAR.B-4676.

Atasoy, F., Açık, E., Gökçen, H., Kırkan, Ş., Yaman, S., Kaya, Y. (2011). Türk Mastifi morfolojik ve genetik özelliklerinin belirlenmesi ve bu köpeğin tanıtılması. Broþür 1. Baskı. Medisan Yayınevi Ltd Şti, Ankara.

Atasoy, F., Kanlı, O. (2005). Türk çoban köpeği kangal. 2. Baskı, No:60. Medisan Yayınevi, Ankara.

Barone, R. (1999). Anatomie comparée des mammifères domestiques. Tome 1: Ostéologie. Vigot Freres, Paris.

Brocal, J., De Decker, S., José López, R., Manzanilla, E. G., Penderis, J., Stalin, C., Gutierrez Quintana, R. (2018). C7 vertebra homeotic transformation in domestic dogs-are Pug dogs breaking mammalian evolutionary constraints? *Journal of Anatomy*. **233 (2):** 255-265.

Cummings, K.R., Vilaplana Grosso, F., Moore, G.E., Rochat, M., Thomovsky, S.A., Bentley, R.T. (2018). Objective measurements of the atlantoaxial joint on radiographs performed without flexion can increase the confidence of diagnosis of atlantoaxial instability in toy breed dogs. Veterinary Radiologyand Ultrasound. **59(6):** 667-676.

Da Costa, R. C., Parent, J. M., Holmberg, D. L., Sinclair, D., Monteith, G. (2008). Outcome of medical and surgical treatment in dogs with cervical spondylomyelopathy: 104 cases (1988-2004). *Journal of the American Veterinary Medical Association*. **233(8):** 1284-1290.

Derakhshi, P., Alizadeh, S., Hosseinchi, M. (2024). Evaluation of radiological and anatomical features of cervical vertebrae in adult Persian cat. *Veterinary Medicine and Science*. **10(6):** e70109.

Dyce, K.M., Sack, W.O., Wensing, C.J.G. (2009). Textbook of Veterinary Anatomy-E-Book. Elsevier Health Sciences.

Elasan, S., Yilmaz, O. (2021). Morphometric and volumetric analysis of the cervical spinal cord and vertebral canal using computed tomography images in normal Van cats. Anatomia, Histologia, *Embryologia*. **50(5):** 826-838.

Evans, H.E., De Lahunta, A. (2012). Miller's anatomy of the Dog-E-Book: Miller's anatomy of the Dog-E-Book. Elsevier Health Sciences.

Falzone, C., Tranquillo, V., Gasparinetti, N. (2022). Comparison of two surgical techniques for the treatment of canine disc associated-cervical spondylomyelopathy. *Frontiers in Veterinary Science*. **9:** 880018.

Fedorov, A., Beichel, R., Kalpathy-Cramer, J., Finet, J., Fillion-Robin, J.C., Pujol, S., Bauer, C., Jennings, D., Fennessy, F.M., Sonka, M., Buatti, J., Aylward, S.R., Miller, J.V., Pieper, S., Kikinis, R. (2012). 3D Slicer as an image computing platform for the quantitative imaging network. *Magnetic Resonance Imaging.* **30(9):** 1323-1341.

Fidan, M.A. (2023). Aksaray malaklı köpeklerinde lumbal ve sakral vertebraların morfometrik olarak incelenmesi. Master's thesis, Aksaray Üniversitesi Sağlık Bilimleri Enstitüsü.

Fidan, M. A., Özüdoğru, Z. and ilgün, R. (2024). Macro-anatomical investigations on the plexus lumbosacralis of the aksaray malakli dog. *Iranian Journal of Veterinary Medicine.* **18(1).**

Fidancı, S.G. and Orhan, I. (2025). The role of 3D laser scanning and printing in veterinary anatomy education: A study on feline scapula and humerus. *Indian Journal of Animal Research*. **59(9):** 1593-1598. doi: 10.18805/IJAR.BF-1986.

Fourie, S.L., Kirberger, R.M. (1999). Relationship of cervical spinal cord diameter to vertebral dimensions: A radiographic study of normal dogs. *Veterinary Radiology and Ultrasound*. **40(2):** 137-143.

Friess, M. (2012). Scratching the surface? The use of surface scanning in physical and paleoanthropology. *Journal of Anthropological Sciences*. **90(1):** 1-25.

Gelati, G., Tanga, M. (2015). Morphometry and laser scanner imaging: A revolution in Anatomy. *Journal of the Siena Academy of Sciences*. **7(1).** doi: 10.4081/jsas.2015.6416.

Hildebrand, T. (2019). Comparative assessment of anatomical details of thoracic limb using 3D modeling. *Journal of Veterinary Anatomy.* **73(1):** 50-59.

İlgün, R., Özkan, Z. E., Yılmaz, S., Karan, M. (2017). Aksaray Malaklı köpeklerinde columna vertebralis'in makro-anatomik olarak incelenmesi. **31(2):** 117-121.

İlgün, R., Özüdoğru, Z., Karabulut, O., Can, M. (2022). Macroanatomical and morphometric study on the skull bones of Aksaray Malakli dogs. *Folia Morphologica*. **81(1):** 157-163.

İnanç, M.E., Tekin, K., Olgac, K.T., Yilmaz, B., Cil, B., Tasdemir, U., Uysal, O. (2018). Effect of cholesterol loaded cyclodextrin on semen cryopreservation of Aksaray Malakli shepherd dogs of different ages. *Animal Reproduction Science*. **193:** 191-200.

Kalantar, S.B. (2013). Fractures of the C1 and C2 vertebrae. *In Seminars in Spine Surgery*. **25(1):** 23-35.

Kim, D., Chang, D., Kim, G. (2022). Radiographic evaluation of atlas and axis anomalies in toy breed dogs with and without atlantoaxial subluxation. *In vivo*. **36(6):** 2751-2755.

König, H.E., Bragulla, H. (2007). Veterinary anatomy of domestic mammals: Textbook and colour atlas. Schattauer Verlag.

Lievens, M., De Kock, L., Ureel, M., Villeirs, G., Van Paepegem, W. and Coopman, R. (2025). The accuracy of an optical white light desktop 3D scanner and cone beam CT scanner compared to a multi-slice CT scanner to digitize anatomical 3D models: A pilot study. *Craniomaxillofacial Trauma and Reconstruction*. **18(2):** 27.

Longo, F., Nicetto, T., Banzato, T., Savio, G., Drigo, M., Meneghello, R., Isola, M. (2018). Automated computation of femoral angles in dogs from three-dimensional computed tomography reconstructions: Comparison with manual techniques. *The Veterinary Journal*. **232:** 6-12.

McGraw, K.O., Wong, S.P. (1996). Forming inferences about some intraclass correlation coefficients. *Psychological Methods*. **1(1):** 30.

Özkadif, S., Halıgür, A. (2019). Tilki (*Vulpes vulpes*) cervical vertebrae'nın morfometrik özelliklerinin üç boyutlu rekonstrüksiyon kullanarak incelenmesi. *Veterinary Journal of Mehmet Akif Ersoy University*. **4(2):** 57-61.

Özkadif, S., Haligur, A., Eken, E. (2019). A three-dimensional reconstruction of the scapula in the red fox (*Vulpes vulpes*). *Indian Journal of Animal Research.* **53(3):** 336-340. doi: 10.18805/ijar.B-987.

Özüdoğru, Z., Fidan, M.A., Gümüş, F., ilgün, R. (2023). Aksaray Malaklı köpeklerinde tibia ve interkondiler geniþlik indeksi üzerine morfometrik bir çalıþma. *Journal of Advances in VetBio Science and Techniques.* **8(2):** 143-149.

Planchamp, B., Bluteau, J., Stoffel, M.H., Precht, C., Schmidli, F., Forterre, F. (2020). Morphometric and functional study of the canine atlantoaxial joint. *Research in Veterinary Science*. **128:** 76-85.

Planchamp, B., Forterre, F., Vidondo, B., Hernandez Guerra, A.M., Plessas, I.N., Schmidt, M.J., Precht, C. (2022). Determination of cutoff values on computed tomography and magnetic resonance images for the diagnosis of atlantoaxial instability in small breed dogs. *Veterinary Surgery*. **51(4):** 620-630.

Prameela, M.D., Prabhu, L.V., Murlimanju, B.V., Pai, M.M., Rai, R., Kumar, C.G. (2020). Anatomical dimensions of the typical cervical vertebrae and their clinical implications. *European Journal of Anatomy*. **24(1):** 9-15.

Smith, R., Jones, L. (2016). Determination of cutoff values for atlantoaxial instability on CT in dogs. *Veterinary Radiology and Ultrasound*. **57(3):** 245-253.

Şengül, G., Kadıoğlu, H.H. (2006). Morphometric anatomy of the atlas and axis vertebrae. *Turkish Neurosurgery*. **16:** 69-76.

Takahashi, F., Hakozaki, T., Kanno, N., Harada, Y., Yamaguchi, S., Hara, Y. (2017). Evaluation of the dens-to-axis length ratio and dens angle in toy-breed dogs with and without atlantoaxial instability and in healthy Beagles. *American Journal of Veterinary Research.* **78(12):** 1400-1405.

Tominaga, T., Dickman, C. A., Sonntag, V. K., Coons, S. (1995). Comparative anatomy of the baboon and the human cervical spine. *Spine.* **20(2):** 131-137.

Veterinaria, N.A. (2017). Nomina Anatomica Veterinária. International Committee On Veterinary Gross Anatomical Nomenclature. 6th ed. Hannover. pp. 73-147.

Von Den Driesch, A. (1976). A guide to the measurement of animal bones from archaeological sites. Peabody Museum Press.

Waltenberger, L., Rebay Salisbury, K. and Mitteroecker, P. (2021). Three dimensional surface scanning methods in osteology: A topographical and geometric morphometric comparison. *American Journal of Physical Anthropology.* **174(4):** 846-858.

Waxenbaum, J.A., Reddy, V., Black, A.C. and Futterman, B. (2025). Anatomy, Back, Cervical Vertebrae. In: StatPearls. StatPearls Publishing, Treasure Island (FL); PMID: 29083805.

White, D.A., Renberg, W.C., Roush, J.K., Hallman, M.R., Mauler, D.A., Milliken, G.A. (2019). Flexed radiographic angles for determination of atlantoaxial instability in dogs. *Veterinary Surgery*. **48(8):** 1406-1415.

Zehtabvar, O., Vajhi, A.R., Akbarein, H.A., Ahmadian, F.S., Khanamooeiashi, M., Soflaei, R., Borgheie, F. (2022). CT anatomy of cervical vertebrae of Asian elephant (*Elephas maximus*). *Veterinary Medicine and Science.* **8(4):** 1750-1768.

Zibis, A.H., Mitrousias, V., Baxevanidou, K., Hantes, M., Karachalios, T. and Arvanitis, D. (2016). Anatomical variations of the foramen transversarium in cervical vertebrae: Findings, review of the literature and clinical significance during cervical spine surgery. *European Spine Journal*. **25(12):** 4132-4139.